

DAA/LANGLEY

IN-CAT. 20

76298 -CR

SEMI-ANNUAL REPORT

FOR

NASA GRANT - NAG-1-431

P.42

PERIOD: NOVEMBER 1, 1986 - APRIL 30, 1987

(NASA-CR-180975) [INVESTIGATION OF THE  
ACOUSTIC PROPERTIES OF COMPOSITE MATERIALS]  
Semiannual Report, 1 Nov. 1986 - 30 Apr.  
1987 (Christopher Newport Coll.) 42 p  
Avail: NTIS HC A03/MF A01

N87-26973

Unclas  
0076298

CSCL 21H G3/20

PRINCIPAL INVESTIGATOR:

B.T. SMITH

DEPARTMENT OF PHYSICS  
CHRISTOPHER NEWPORT COLLEGE  
NEWPORT NEWS, VIRGINIA 23606

NASA TECHNICAL OFFICER:

J.S. HEYMAN, HEAD, MCIS

NASA/LANGLEY RESEARCH CENTER  
MAIL STOP 231  
HAMPTON, VIRGINIA 23665

This report covers the work done on NASA Grant NAG-1-431 for the period from November 1, 1986 to April 30, 1987. At the beginning of the grant period there arose an opportunity to contribute to the effort to provide inspection of the bondlines in the Space Shuttle Solid Rocket Motor (SRM). The bondlines are defined as the interface between components of the rocket motor, such as, the case, liner, insulation, and propellant. In collaboration with the researchers of the Materials Characterization and Instrumentation Section this research was the focus of the past six months.

The effort in the investigation of the bondlines in the membrane region of the SRM has centered on representative samples provided by Morton/Thiokol. These samples have pull-tabs or in one case grafoil inserts to simulate delaminations at various points in the multilayer structure of steel case, liner, insulation, liner, and propellant. This report will discuss our continuing approach to examining these defects which is predicated on a model of an ultrasonic wave propagating in a lossy multilayer resonant structure, the experimental arrangements used, and the results of these experiments.

## MODEL CONSIDERATIONS

The structure under investigation is the Shuttle SRM, a multilayer resonant structure with lossy components. The steel case reverberates readily since it has very little attenuative loss while the insulation and propellant are very lossy. Therefore, unless one is careful in examining this type of structure the ringing in the steel can mask delaminations in the insulation and propellant bondline regions. Shown in figure 1 is the representative model that we have used to indicate the type of measurements to be made.

We have used a transmission line model which is shown schematically in figure 1. The components of the structure are modeled as individual complex valued impedances in a transmission line (A short discussion of the model can be found in *Methods of Experimental Physics*, Volume 19, edited by Peter D. Edmonds, pp 41-42). The result for a lossy transmission line can be represented as:

$$Z_{in} = Z_0 \{ [Z_1 + Z_0 \tanh(\theta l)] / [Z_0 + Z_1 \tanh(\theta l)] \},$$

where  $\theta = \alpha + ik$ ,  $l$  is the thickness of the layer, and  $k$  is the wave number ( $\omega/c$ ). The complex impedance is solved for successive layers over a range of frequencies (in this case from 0 to 2 MHz); the total frequency response of the multilayer resonator can then be used to calculate the response of the system for various input waves. This is done by convolving the input wave form with the response of the resonant structure. The listing of the program for the model calculation is included in the appendix along with the model parameters that are input. These values used in the calculation were obtained from Titan SRM data; at present we are independently determining the shuttle SRM values from individual specimens provided by Morton/Thiokol.

The results of the model calculation are important to the overall evaluation of the SRM samples provided. Shown in figure 2 is the flow for the investigation of these samples. The model calculation provides the starting point to determine which are the best ultrasonic parameters to measure for a search of delaminations in the bondlines. Figure 2 illustrates that once the characteristics of such a system are predicted, the approach to detecting delaminations at the bondlines can take many forms. The many techniques illustrated in this figure all must be implemented with the limitations of the actual structure taken into account. These limitations are chiefly on the frequency range of the ultrasonic waves being used in these techniques. The results of model calculations and experiments will illustrate this point.

The type of results that can be expected from an experiment can be predicted by the model. We can illustrate this by reviewing the results of a calculation for a specimen with an air gap between the insulation and propellant. The computer generated tone burst of 0.5 MHz is shown in figure 3. This frequency value was picked to match the lowest frequency transducer that we have available at this time. Figure 4 is the frequency response for a multilayer resonator of 2" of water, 0.5" of steel, 0.1" of insulation, and 4.0" of propellant. The resonance points are the only frequencies where appreciable energy is coupled into the total structure; thus the choice of frequency for the input wave is very important. The dotted lines correspond to the calculation which includes a 0.030" air gap between the insulation and the propellant. The convolution of the resonator response and the input wave yields the observed wave form for such a system. Shown in figure 5 is the resulting wave form for the configuration without an air gap. The middle figure is the spectral response of the wave after a windowing operation is performed from channel 400 to channel 800. This windowing operation improves

the signal to noise. Thus we only include that part of the wave of interest which comes after the front surface reflection and deeper down in the model structure. We call that the resonance decay technique. The bottom part of the figure is the response of the resonant structure. In figure 6 is the same calculations for a structure with an air gap between the insulation and propellant. A comparison between the top wave forms in figures 5 and 6 shows that the actual amplitude differences in the wave excluding the front surface reflection are sufficient to image the air gap. The comparison in figure 7 shows the spectral magnitude differences between the two wave forms windowed over the same channel numbers (400 to 800). The difference is very noticeable. The shift in frequency of the peak is also evident for the change in the resonant structure by adding an air gap. The differences in the resonant structures model is shown in figure 8; it is clear that only some frequencies can probe the structure for defects. In fact for the case of the 0.1" thick insulation there are different techniques (all related) that can image a delamination by processing the resonance decay wave. For a given input, either single pulse or tone burst, an examination of the frequency content or for a tone burst input the peak amplitude of the received wave can image a delamination.

For a model with a thicker layer of insulation (0.5") the level of detectability for a 500 kHz wave input is much lower. The same calculation with a 0.5" layer of insulation is shown in figure 9 for no air gap and in figure 10 for an air gap between the insulation and propellant. The differences between the wave forms are undetectable when comparing the top figures in figure 9 and 10. In figure 11 the spectral response for both structures are shown for a window from channel 400 to channel 800. The difference only exists at the peak and is only about 13 percent. The differences in the resonant structure response is shown in figure 12. The response in figure 12 near 500 kHz is down by a factor of 300 compared to the result for 0.1" insulation; even at a frequency of 220 kHz the response is down by a factor of 13 for the same comparison. The actual data will illustrate that the detectability of defects with a probing frequency of 500 kHz, using the techniques discussed in this report, is limited to thin insulation thickness at the present time.

## Experimental Procedures

The experiments were performed in a water bath with a broadband damped transducer with a nominal center frequency of 500 kHz. A computer controlled scanning bridge was employed to scan the samples. The experimental arrangements are shown in figures 13 and 14. The different techniques shown in these figures concentrated on examining the energy returned in the resonance decay.

The first arrangement is shown in figure 13. A sampled continuous wave is generated by gating the tracking generator output of a spectrum analyzer into the transducer and then gating the reflected wave into the spectrum analyzer. The reflection is gated to only include that part of the wave past the front surface reflection. The entire spectrum can be stored on the computer for later analysis or the spectrum analyzer can be set up to output only one frequency and the video output can be acquired, read with a digital voltmeter and input into a computer along with the coordinates of the transducer to construct an image of the sample and delamination. This arrangement is similar to a tone burst input to the transducer with the appropriate processing of the reflected wave.

The experimental arrangement shown in figure 14 was used for most of the results reported here. The wave input to the transducer can either be a tone burst or a pulse. The tone burst was generated with a HP3314 function generator capable of delivering a sine wave tone burst of any frequency, amplitude, or extent. The pulse was supplied by a Metrotek MP 215 pulser. The input and received wave were coupled to the transducer by a diode clipper circuit. The reflected wave can be analyzed by various techniques. The wave could be gated to include the bondline regions and then peak detected to make an image of the amplitude as a function of position. The wave can also be input to a digitizer (Data Precision 6000) for post processing. The post processing can be similar to that described in the model calculations. The frequency content or integrated energy contained in some region of the reflected wave can be used to image the specimen. In all cases the data was input to a computer for later analysis and display on an image analyzer.

## Experimental Results

The first specimen examined is shown schematically in figure 15. This sample is a flat steel plate with insulation bonded to it. Grafoil inserts were included to simulate delaminations of various sizes. The grafoil was placed both in front and behind a liner material which makes the bond between the steel and insulation. The liner material was also varied in thickness to simulate the range of values usually present in the manufacture of the SRM.

A pulse echo technique was used with a 5 MHz transducer and peak detection of the tenth reverberation between the face of the transducer and the specimen. The transducer had a focus length of 4.0" and an aperture of 0.5". Such a high frequency was possible in this case because the delamination was essentially directly behind the steel layer and the return is directly dependent on the amount of energy coupled to the insulation layer. The effect of the liner is small because of its thinness. Figure 16 shows the result of the scan over a range of 60x20 centimeters with a step size of 0.2 centimeters. The image has been cast in grey scale to represent the relative amplitude of the reflected wave. The scale has a range of 27 dB from low values in black to high values in white. The white shapes of the inserts are well resolved in this scan. At the delamination the reflected signal is larger than elsewhere since all the energy is reflected back and not coupled into the lossy insulation layer. The fuzzy shape for the inserts behind the liner may be due to attenuation of the wave in the liner or diffraction effects in the liner. It was possible to use a high frequency transducer in this case since the steel is not very lossy and we were examining a bondline just behind the steel. For examinations of the insulation / propellant bondline this is not the case since the materials are very attenuating even at low frequencies.

The second sample examined was Sample 8-1 which is shown in figure 17. This particular sample was examined with several techniques. For this and the following experiments the transducer used was a broadband highly damped transducer with a nominal center frequency of 500 kHz, a 2.0" focal length, and an aperture of 1.125 inches. Shown in figure 18 is a scan generated from the output of the video signal from the spectrum analyzer when the tracking generator is fixed at 500 kHz. The reflected signal was gated into the spectrum analyzer so as to include the internal bondlines. The scan size was 8x12 centimeters with a 0.2 centimeter stepsize. The triangular shaped delamination is well evident.

A similar technique to the above is accomplished by inputting a tone burst to the transducer. In figure 19 the result is shown for a tone burst of 10 cycles of a 500 kHz sine wave which was amplified by an ENI 3100L power amplifier. The reflected wave was peak detected in the resonance decay region and the resulting amplitude measured is shown as a relative grey scale image over a range of 22 dB in figure 19. The scan size was 9x15.5 centimeters with a step size of 0.25 centimeters. The delamination is well resolved.

To test other possible techniques the above experiment, where a 500 kHz tone burst was used as the input wave, was repeated with the output now being digitized for post processing. The data was sampled over 256 points with a sampling frequency of 5 MHz. One of the waveforms that was digitized is shown in figure 20. The delay was set to exclude part of the front surface reflection, allowing greater amplification of the later part of the wave. The wave was windowed from channel number 150 to 250, and this resulting wave was input to an FFT for the spectral response which is shown in figure 21. The solid line is the result for x-y position 1,1 and the dotted line corresponds to position 16,21 which is over the delamination. The peak is much smaller over the delamination and is shifted similar to the result of the model calculation in figure 7. The relative differences between the model and the experiment are not commensurate but as noted previously the values input to the model calculation are being remeasured. This is the same analysis discussed in the model calculation section. This approach was repeated for all the data, which was windowed to include only the contributions from the bondline region, then a fast Fourier transform (FFT) was taken and the spectra over a range from 0.45 to 0.52 MHz was integrated to arrive at a number representative of the energy returned from that location on the sample. Again, the delamination appearing in figure 22 is well resolved and exhibits a relative range of 14 dB.

The test was again repeated for a pulse input to the transducer rather than a tone burst. This approach is the normal mode of testing with most commercial NDE systems. The result of the digitization and same post processing is shown in figure 23. While, the result of the peak detection is shown in figure 24. A pulse driven broadband transducer responds differently than a tone burst driven transducer. A tone burst provides energy in only a narrow frequency band while a pulse will promote a broadband response in the transducer. In the discussion of the model calculation it was noted that the

energy input to the resonant structure is only efficient over a narrow band of frequencies. Therefore a pulse input is an inefficient way to examine this structure since it puts energy in frequency bands which do not provide an internal view of the structure. This is the probable cause of the spectral analysis in figure 23 having less resolution than figure 19. In the case of the peak detected scan of figure 24, the signal to noise is insufficient to resolve any delamination indication. Figure 23 exhibits a relative range of 12.6 dB while figure 24 exhibits a range of 7.6 dB. Further, since pulse echo techniques are the normal mode of testing with most commercial NDE systems, it is clear that an advanced NDE inspection is necessary using frequency domain approaches.

Sample 4-1 was also examined. This sample has an insulation thickness of 0.5" and the delamination after the insulation and before the liner-propellant. The first technique shown on the top of figure 25 and labeled 'L' is the result of a scan using the spectrum analyzer set at 500 kHz and using the video out as the detected signal. The bottom of figure 25 labeled 'I' is the image developed from signal processing the digitized wave form from a reflected tone burst with a frequency of 500 kHz. The digitized wave was windowed, an FFT was taken, and the magnitude over a frequency range of 0.48 to 0.52 MHz was integrated and used to create the grey scale image. Although both images give some indication of damage at the approximate location of the delamination the view is not well resolved. Recall in the model calculation that the possible response at this frequency is very small compared to that for only a 0.1" thick insulation sample. Much better penetration can be expected for lower frequency input waves.

## Conclusions

This report has given a short review of the work completed to date on the investigation of the bondline integrity in the membrane region of the SRM. The model calculations clearly point the way for the investigation. The need for low frequency transducers has been demonstrated in both the model and experimental results. The need to use probing techniques which make effective use of the frequency windows open to the internal structure is also evident from the theory and experiment. There are a number of samples that have been received and still need to be examined.

# APPENDIX

The following is a program written in Fortran to run on a VAX 750 that calculates the frequency response of a multi-component transmission line with lossy components.

```

c written by W.P. Winfree
c modified by B.T. Smith
C*****
C calculates the reflection from up to 20 layers

C properties of layers in/out from file

C does calculation in the frequency domain from a lower frequency to higher
C frequency range
C*****
C  Implicit None
      Integer I, Npts_fft, Number_layers
C Npts_fft - number of points in fft
C  Parameter ( Npts_fft = 1024 )

      Real Min_freq, Max_freq, Pi, F, Thickness
C Max_freq - Maximum frequency of fourier transform
c  Parameter ( Min_freq = 3.00E5 )
c  Parameter ( Max_freq = 4.0E5 )

      Real Real_part, Imag_part, ArcTangent
      Complex Data( 2048 ), Reflection,XC(2048),DATA1(2048),XC1(2048)
      Real Phase(2048), Freq(2048)
      Character Output_file*40, Input_file*40,FILENAMEA*40
      INTEGER*2 INDEX,CHAN1,CHAN2
      REAL XR(2048),D(2048),R(2048),IMAG(2048),D1(2048),R1(2048)
      DIMENSION DSYS(2048),XI(4096)
      INTEGER*4 XSIZE,YSIZE,NO_BYTES
      CHARACTER*1 ANS
      CALL CMDLIN ('DEV VW SIZE 7,13 ERASE')

***INPUT SYSTEM RESPONSE*****
      TYPE *, 'INPUT THE NAME OF SYSTEM RESPONSE FILE'
      ACCEPT '(A)',FILENAMEA
      TYPE *, 'INPUT SAMPLE FREQUENCY OF INPUT'
      ACCEPT *,SFREQ
100 CONTINUE

      OPEN(UNIT=10,FILE=FILENAMEA,READONLY,
      1 STATUS='OLD',FORM='UNFORMATTED')
      READ(10)XSIZE,YSIZE,NO_BYTES
      TYPE *, 'X= ',XSIZE,' Y= ',YSIZE,' # = ',NO_BYTES
      READ(10) (DSYS(I),I=1,NO_BYTES)
      CLOSE (10)

      IF(NO_BYTES .NE. 1024) THEN
        DO I=NO_BYTES+1,1024
          DSYS(I)=0.0
        
```

```

        END DO

        NO_BYTES=1024
    END IF

    *****

    Write ( 6, '(a)' ) '$Minimum and maximum frequency : '
    Read ( 5, * ) Min_freq, Max_freq
    Min_freq = Min_freq*1.e6
    Max_freq = Max_freq*1.e6

    *****PROPERTIES FILES WITH AND WITHOUT AIR GAPS*****

    Write ( 6, '(a)' ) '$Properties File WITH NO AIR GAP: '
    Read ( 5, '(a)' ) Input_file
    Open ( Unit = 3, File = Input_file, Status = 'Old', ReadOnly )

    Call Get_properties ( Number_layers )

    Close ( Unit = 3 )

    NPTS_FFT=NO_BYTES

    F = Min_freq
    C calculate response in frequency domain
    Do I = 1, Npts_fft/2+1

        Data(I) = Reflection(f, Number_layers )
        F = F + (Max_freq - Min_freq) /( Npts_fft-1 )

    End do
    *****
    Write ( 6, '(a)' ) '$Properties File WITH AIR GAP: '
    Read ( 5, '(a)' ) Input_file
    Open ( Unit = 3, File = Input_file, Status = 'Old', ReadOnly )

    Call Get_properties ( Number_layers )

    Close ( Unit = 3 )

    NPTS_FFT=NO_BYTES

    F = Min_freq
    C calculate response in frequency domain
    Do I = 1, Npts_fft/2+1

        Data1(I) = Reflection(f, Number_layers )
        F = F + (Max_freq - Min_freq) /( Npts_fft-1 )

    End do

    *****

    F= Min_freq
    Do I = 1, Npts_fft/2+1

```

# C frequency domain output

```

      Freq (I) = F*1.e-6
      D(I)=CABS (DATA(I))
      D1(I)=CABS (DATA1(I))
      XR(I)=F*1.E-6

      F = F + (Max_freq - Min_freq) /( Npts_fft-1 )
End do

*****
DO I=1,NO_BYTES
      XI(I)=I
END DO

*****CALCULATE FFT OF SYSTEM RESPONSE*****
TYPE *, 'INPUT ANY CUTOFF FOR SYSTEM INPUT'
CALL CMDLIN('XTITLE CHANNEL YTITLE AMP.')
CALL GENPLT(XI,DSYS,NO_BYTES)
TYPE *, 'INPUT CHANNELS FOR CUTOFF OF SYSTEM INPUT'
ACCEPT *,CHAN1,CHAN2

DO I=1,CHAN1
      DSYS(I)=DSYS(I)*EXP(-(I-CHAN1)**2/20.)
END DO

DO I=CHAN2,NO_BYTES
      DSYS(I)=DSYS(I)*EXP(-(I-CHAN2)**2/20.)
END DO

CALL CARRAY (DSYS,XC,NO_BYTES)
CALL SFFT(XC,NO_BYTES,-1)
*****
*** CONVOLVE THE SYSTEM INPUT WITH RESPONSE
*****

DO I=1,NO_BYTES/2+1
      XC1(I)=XC(I)
      XC(I)=DATA(I)*XC(I)
      XC1(I)=DATA1(I)*XC1(I)

      IF (I .NE. 1 .AND. I .NE. NO_BYTES/2+1) THEN
            XC(NO_BYTES+2-I)=CONJG(XC(I))
            XC1(NO_BYTES+2-I)=CONJG(XC1(I))
      ELSE
            XC(I)=REAL(XC(I))
            XC1(I)=REAL(XC1(I))
      END IF
END DO

*****

CALL SFFT(XC,NPTS_FFT,1)
CALL RARRAY(R,XC,NPTS_FFT)

CALL SFFT(XC1,NPTS_FFT,1)
CALL RARRAY(R1,XC1,NPTS_FFT)

```

```

*****FFT OF RESULT*****
CALL CMDLIN('XTITLE CHANNEL YTITLE AMPLITUDE PLOT')
CALL GENPLT(XI,R,NPTS_FFT)
TYPE *,'INPUT CHANNELS FOR CUTOFF OF OUTPUT OF CONVOLUTION'
ACCEPT *,CHAN1,CHAN2

DO I=1,CHAN1
    R(I)=R(I)*EXP(-(I-CHAN1)**2/20.)
    R1(I)=R1(I)*EXP(-(I-CHAN1)**2/20.)
END DO

DO I=CHAN2,NO_BYTES
    R(I)=R(I)*EXP(-(I-CHAN2)**2/20.)
    R1(I)=R1(I)*EXP(-(I-CHAN2)**2/20.)
END DO

    DELF=(SFREQ*1E6)/NO_BYTES
DO I=1,NO_BYTES

    XR(I)=I*DELF
END DO


CALL CARRAY (R,XC,NO_BYTES)
CALL SFFT(XC,NO_BYTES,-1)
CALL AARRAY(R,XC,NO_BYTES)

CALL CARRAY (R1,XC1,NO_BYTES)
CALL SFFT(XC1,NO_BYTES,-1)
CALL AARRAY(R1,XC1,NO_BYTES)

CALL CMDLIN('XTITLE MHZ YTITLE MAG PLOT ')
CALL GENPLT(XR,R,NPTS_FFT/2)

CALL CMDLIN('LTYPE 2 OVERLAY LTYPE 1')
CALL GENPLT(XR,R1,NPTS_FFT/2)

DO I=1,NPTS_FFT/2
    R(I)=R(I)-R1(I)
END DO

CALL CMDLIN('XTITLE MHZ YTITLE DIFFERENCE PLOT')
CALL GENPLT(XR,R,NPTS_FFT/2)

*****SPECTRAL RESPONSE OF MULTILAYER RESONATOR*****
CALL CMDLIN('XTITLE MHZ YTITLE MAG PLOT')
CALL GENPLT(FREQ,D,NPTS_FFT/2)

CALL CMDLIN('LTYPE 2 OVERLAY LTYPE 1')
CALL GENPLT(FREQ,D1,NPTS_FFT/2)

DO I=1,NPTS_FFT/2
    D(I)=D(I)-D1(I)
END DO

CALL CMDLIN('XTITLE MHZ YTITLE DIFFERENCE PLOT')

```

```

CALL GENPLT(FREQ,D,NPTS_FFT/2)
*****

TYPE*, 'INPUT ANOTHER PROPERTY FILE (YES=Y)'
ACCEPT '(A)',ANS
IF(ANS .EQ. 'Y' .OR. ANS .EQ. 'y')GO TO 100

CALL GENOFF

End

C
Complex Function Reflection(f, Number_layers)

Implicit None

Real Pi
Parameter ( Pi = 3.1415927 )

Real D_layer, Rho_layer, Velocity_layer, A_layer
Complex Z_layer
C D_layer- layer thicknss
C Rho_layer - Density of layer
C Velocity_layer - velocity in layer
C Z_layer - acoustic impedance of layer
C A_layer-attenuation layer

Complex Cexp, Conjg, Cmplx,
1 Z_trans, ! function for calculating line Z
2 Z_trans_layer,
! transmission line Z of layer
5 Z_load ! terminating acoustic load
Real F, W, Sinc, C_p_constant, Phi_constant
c f - frequency
C W - angular frequency
Integer Number_layers
! number of layers from input file
Integer Layer ! number of current layer for calculation

If ( F .eq. 0. ) Then
    Reflection = 0.
    Return
End if

W = 6.283185 * F
c find terminating Z
Call Properties_layer ( D_layer, Rho_layer,
1 Velocity_layer, Z_layer, A_layer, F, Number_layers )
Z_load = Z_layer

C find effective Z for all of the layers starting from the
C back layer
Do Layer = Number_layers - 1, 2, -1
    Call Properties_layer ( D_layer, Rho_layer,
1 Velocity_layer, Z_layer, A_layer, F, Layer )
    Z_load = Z_trans ( W, Velocity_layer, A_layer,
1 Z_layer, Z_load, D_layer )

```

```

End do

C find reflection at front layer
  Call Properties_layer ( D_layer, Rho_layer,
    1      Velocity_layer, Z_layer, A_layer, F, 1 )

  Reflection = ( Z_load - Z_layer ) / ( Z_load + Z_layer )

  Return
End

C
Complex function Z_trans ( W, V, A, Z_0, Z_L, L )
  Implicit None
C W - angular frequency
C V acoustic velocity in line
C A - attenuation in line
C Z_0 - acoustic impedance of line
C Z_L - load impedance at end of line
C L - Length of line
  Complex Theta, Ctanh, Cmplx, Z_1
C Theta - complex wave number
C Ctanh - complex hyperbolic tangent
  Real K, L, W, V, A
  Complex Z_0
C K - real part of wave number
  K = W/V
  Theta = Cmplx ( A, K )
  Z_trans = Ctanh ( Theta * L )
  Z_trans = Z_0 * ( Z_L + Z_0 * Z_trans ) /
    1      ( Z_0 + Z_L * Z_trans )

  Return
End

C
Subroutine Get_Properties ( Number_layers )

  Implicit None

  Integer Max_layers ! maximum number of layers in sequence
    ! appears here and Properties_layer
  Parameter ( Max_layers = 20 )

  Real V( Max_layers ), Rho( Max_layers ), T( Max_layers ),
    1      A_constant( Max_layers ), Power( Max_layers )
C V - velocity of each layer
C Rho - density of each layer
C T - thickness of each layer
C A_constant and Power - used to calculate the attenuation of each layer
C      Attenuation = A_constant * Frequency**Power

  Common V, Rho, T, A_constant, Power

  Integer Number_layers

  Number_layers = 1

  Do While ( .true. )
    Read ( 3, *, End = 99 ) V ( Number_layers )
    Read ( 3, *, End = 99 ) Rho ( Number_layers )

```

```

        Read ( 3, *, End = 99 ) T ( Number_layers )
        Read ( 3, *, End = 99 ) A_constant ( Number_layers ),
1
        Power ( Number_layers )
        Number_layers = Number_layers + 1
End do

99 Continue

Number_layers = Number_layers - 1

Return
End

C
Subroutine Properties_layer ( D_layer, Rho_layer,
1      Velocity_layer, Z_layer, A_layer, F, Layer )

    Implicit None
C layer properties
    Real D_layer, Rho_layer, Velocity_layer, A_layer, F,
    1      A_layer_constant
    Complex Z_layer, Cmplx
C D_layer- layer thickness
C Rho_layer - Density of layer
C Velocity_layer - velocity in layer
C Z_layer - acoustic impedance of layer
C A_layer-attenuation layer
C F - Frequency

    Integer Layer ! number of the layer

    Integer Max_layers ! maximum number of layers in sequence
                        ! appears here and Get_Properties
    Parameter ( Max_layers = 20 )

    Real V( Max_layers ), Rho( Max_layers ), T( Max_layers ),
    1      A_constant( Max_layers ), Power( Max_layers )
C V - velocity of each layer
C Rho - density of each layer
C T - thickness of each layer
C A_constant and Power - used to calculate the attenuation of each layer
C      Attenuation = A_constant * Frequency**Power

    Common V, Rho, T, A_constant, Power

    Real W      !angular frequency

    Velocity_layer = V (Layer)
    ! m/sec
    Rho_layer = Rho
    ( Layer)      ! kg/m**3
    D_layer = T ( Layer ) ! m

    If ( Power (Layer) .eq. 0. ) Then
        A_layer = A_constant ( Layer )
    Else
        A_layer = A_constant ( Layer ) *
    1
    (F*1.e-6)**Power ( Layer )

```

```

End if

C for nonzero attenuation the reflection coefficient is complex

  If ( F .eq. 0. ) Then
C at zero frequency the attenuation must be zero
    Z_layer = Rho_layer * Velocity_layer
  Else
    Z_layer = Rho_layer * Velocity_layer
    W = 6.283185 * F
    Z_layer = Z_layer/Cmplx(1.,Velocity_layer*A_layer/W)
  End if

Return
End

C
Complex Function Ctanh(X)
C complex hyperbolic tangent
Implicit None
Complex X, Cexp, Y

If ( Real ( x ) .gt. 80. ) Then
  Ctanh = 1.
Else
  Y = Cexp(x)
  Ctanh = ( Y - 1./Y ) / ( Y + 1./Y )
End if

Return
End

```

## VALUES INPUT TO PROGRAM

### WATER

1482. water velocity m/sec  
1000. Water density kg/m\*\*3  
.0508 thickness of layer m  
0.025 0. attenuation coefficient and power 1/m

### STEEL

5440. Velocity steel m/sec  
7860. Density steel kg/m\*\*3  
.0127 thickness of layer m  
0.0 0. attenuation coefficient and power

### INSULATION

1800. Velocity insulation(silica) m/sec  
1180. Density insulation kg/m\*\*3  
.00254 Thickness of layer! m  
749.0 1.1049 attenuation coefficient and power

### AIR

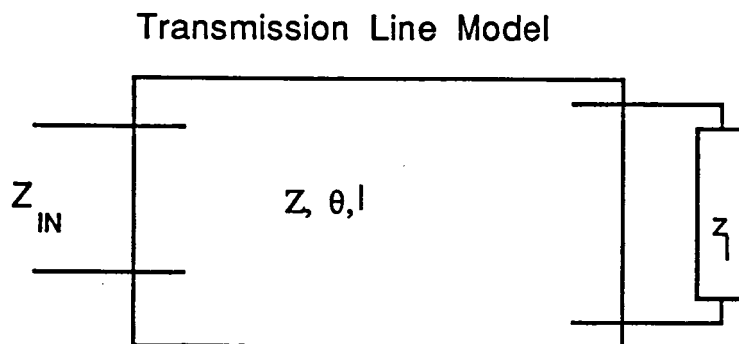
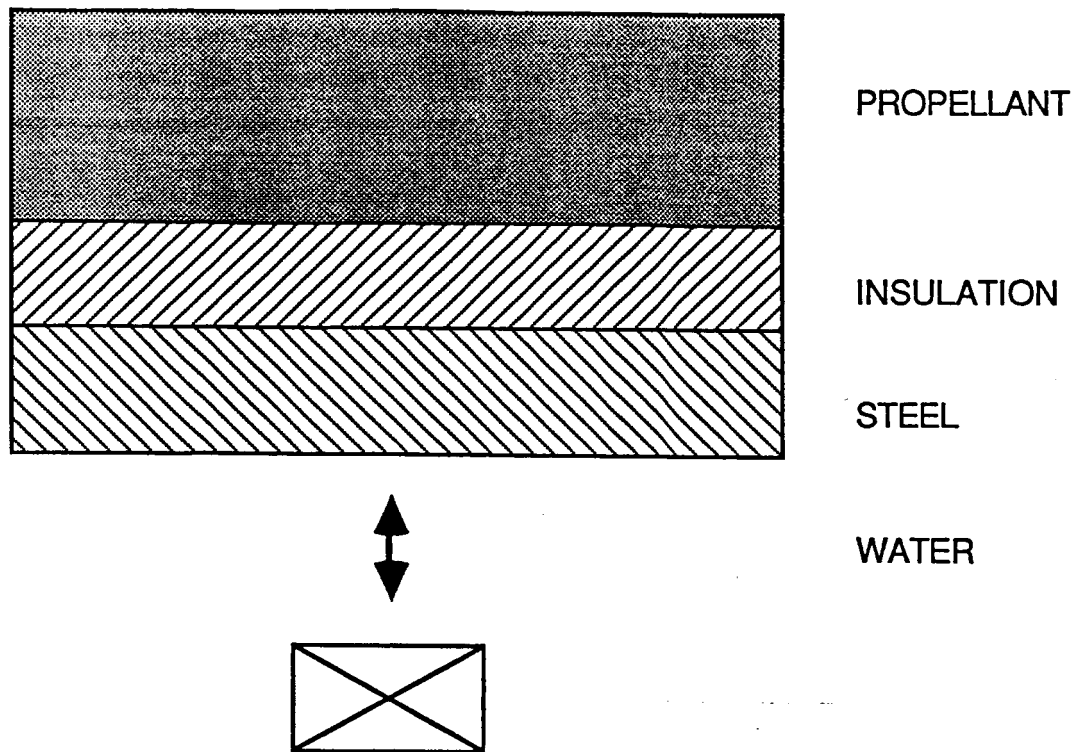
344. VELOCITY OF AIR M/S  
1.2 DENSITY OF AIR KG/M\*\*3  
.000762 THICKNESS OF LAYER M  
4.6 0.0 ATTENUATION(?) AND POWER

### PROPELLANT

2010. Velocity of propellant m/sec  
1770. Density of propellant kg/m\*\*3  
.1016 Thickness of layer m  
191. 0.0 attenuation and power

ORIGINAL PAGE IS  
OF POOR QUALITY

# SRM MODEL CALCULATION



$$\theta = \alpha + ik$$

$$k = \omega/c$$

Figure 1.

# ULTRASONIC NDE RESEARCH

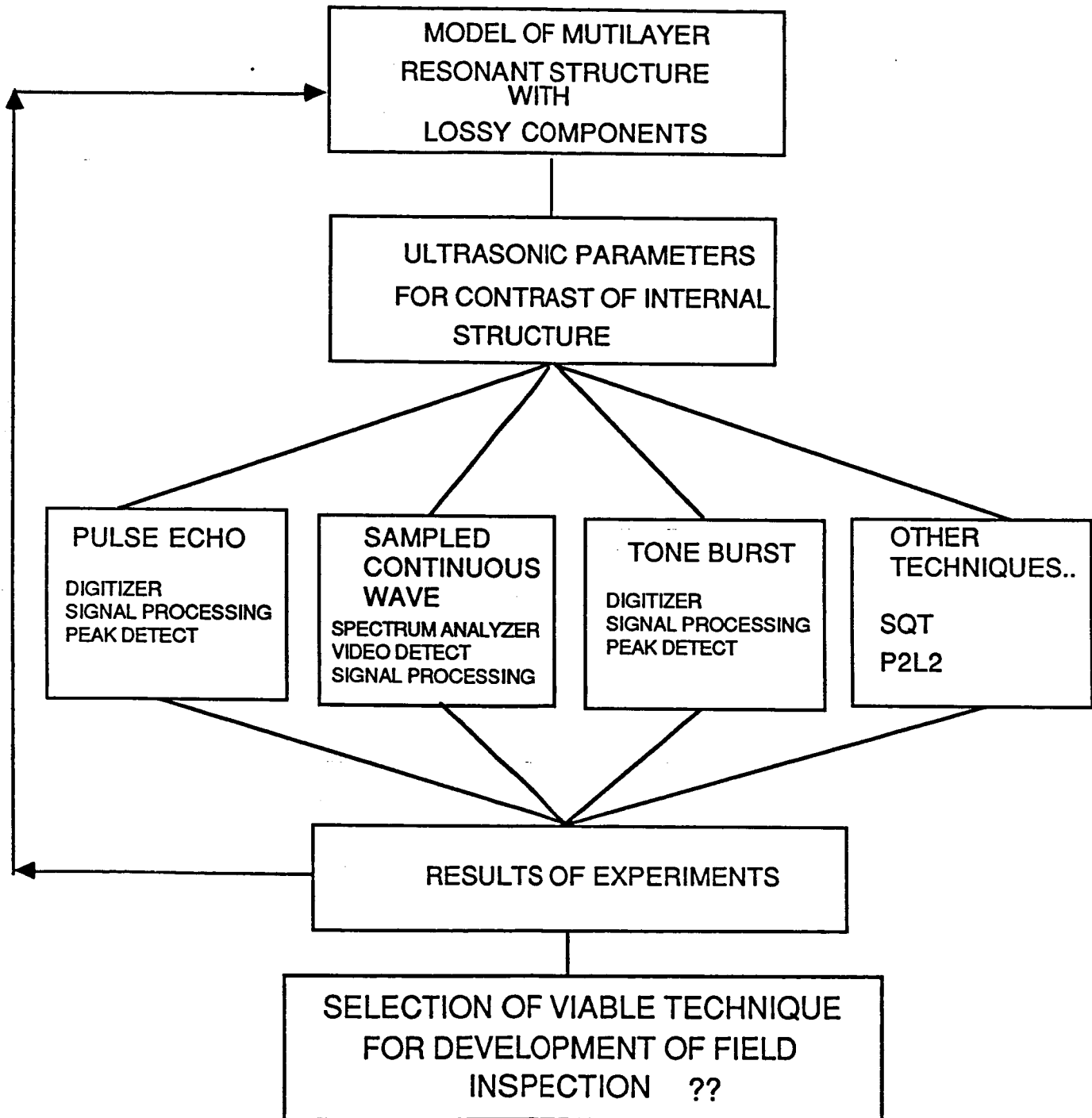
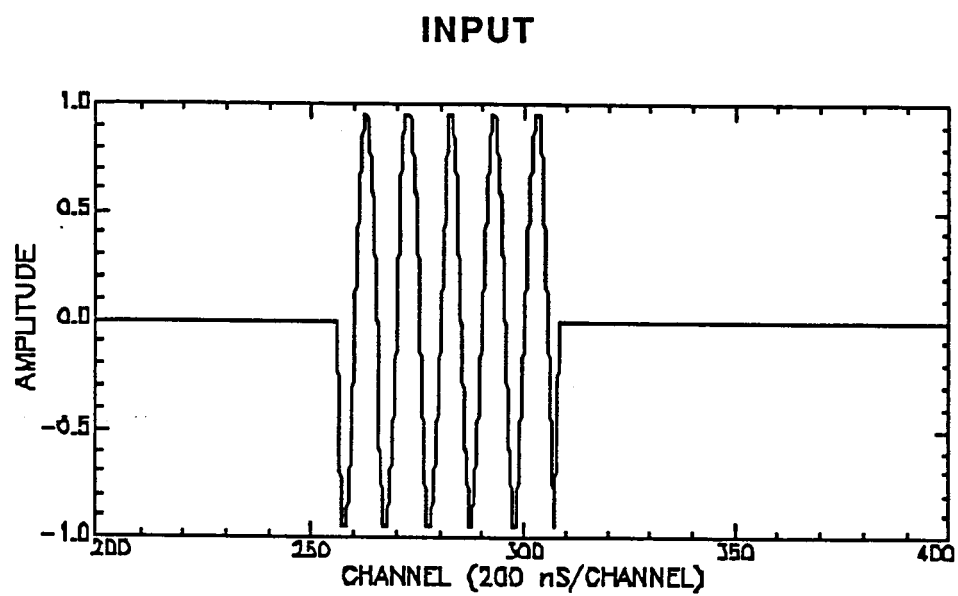


Figure 2.



**Figure 3.**

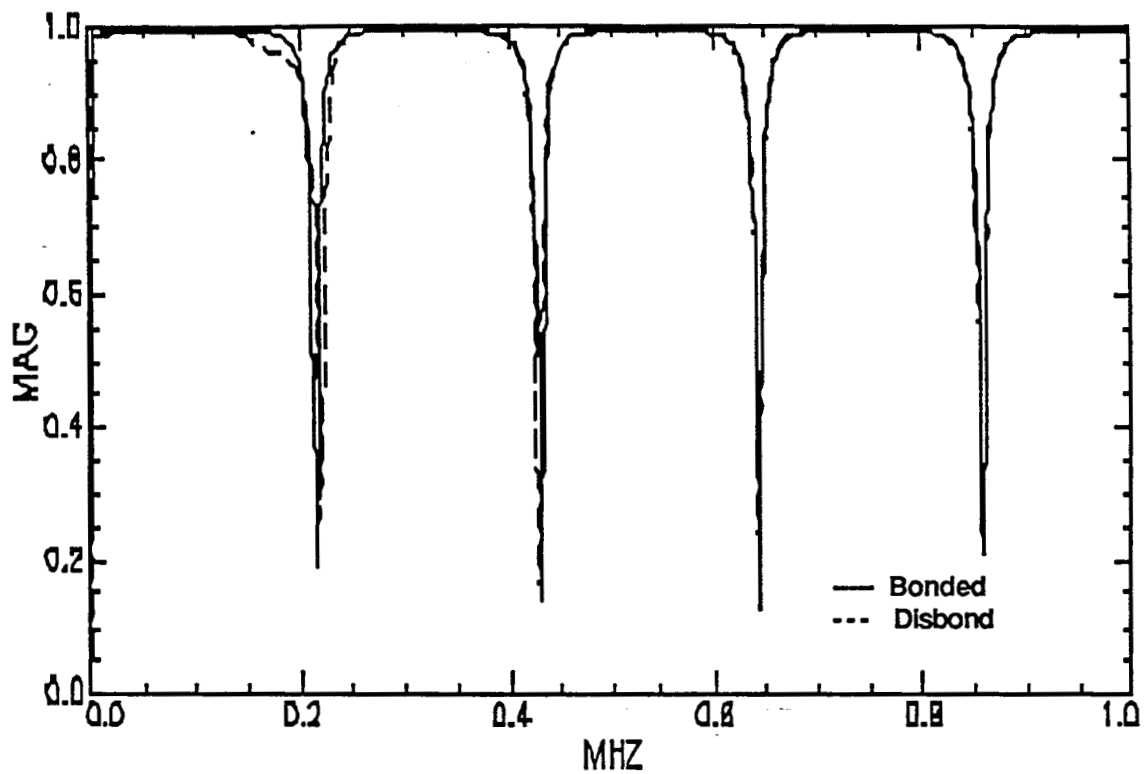


Figure 4. Frequency response of multilayer resonator with bond (—) and disbond (---) between insulator (0.1") and propellant.

# MODEL WITH BOND BETWEEN INSULATION (0.1") AND PROPELLANT

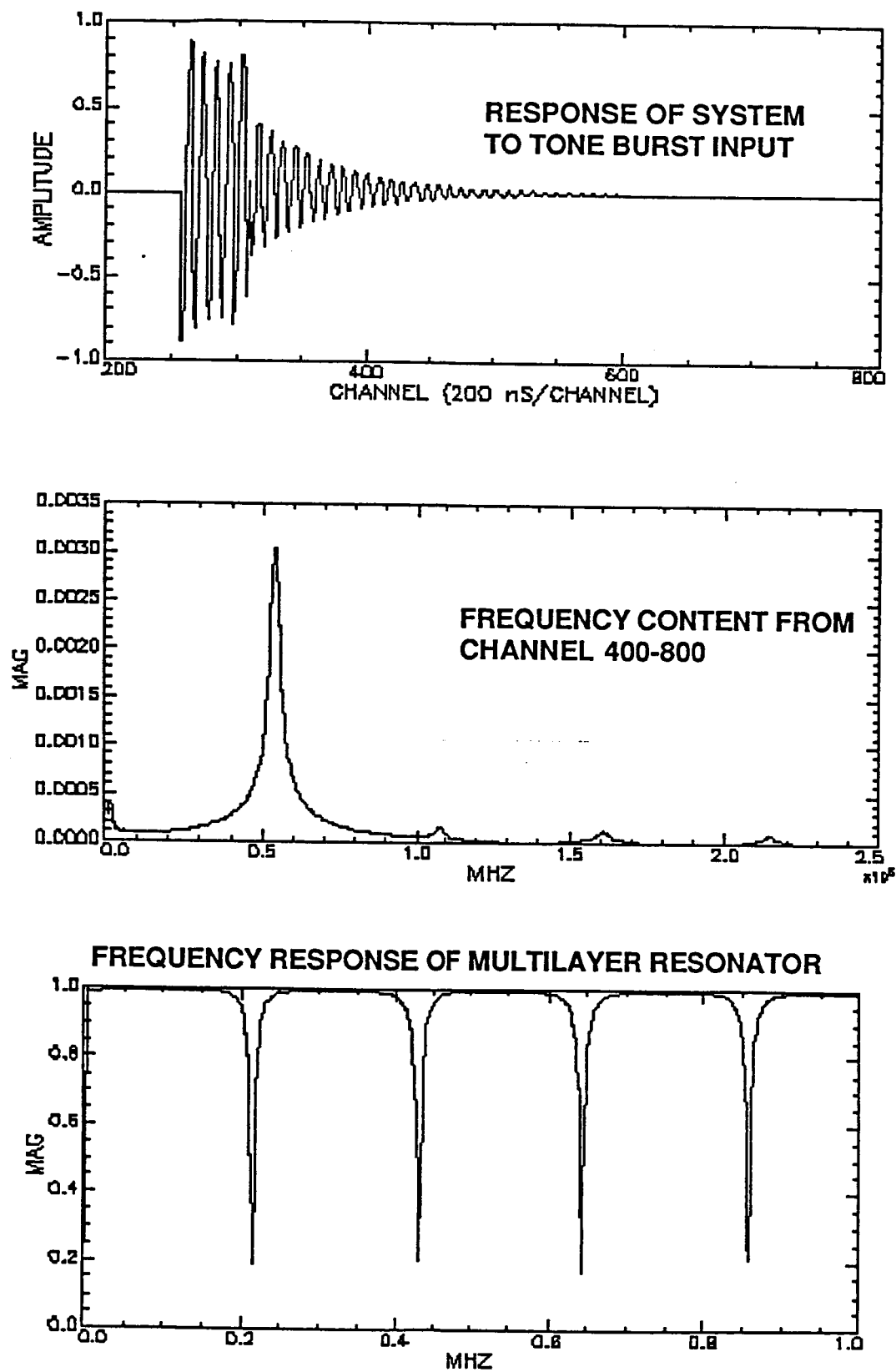


Figure 5.

# MODEL WITH DISBOND BETWEEN INSULATION (0.1") AND PROPELLANT

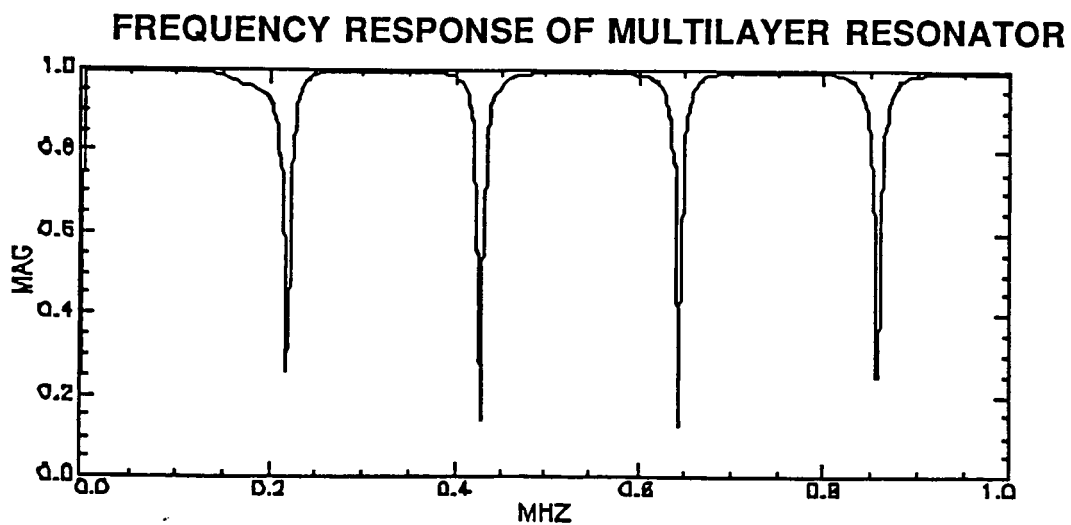
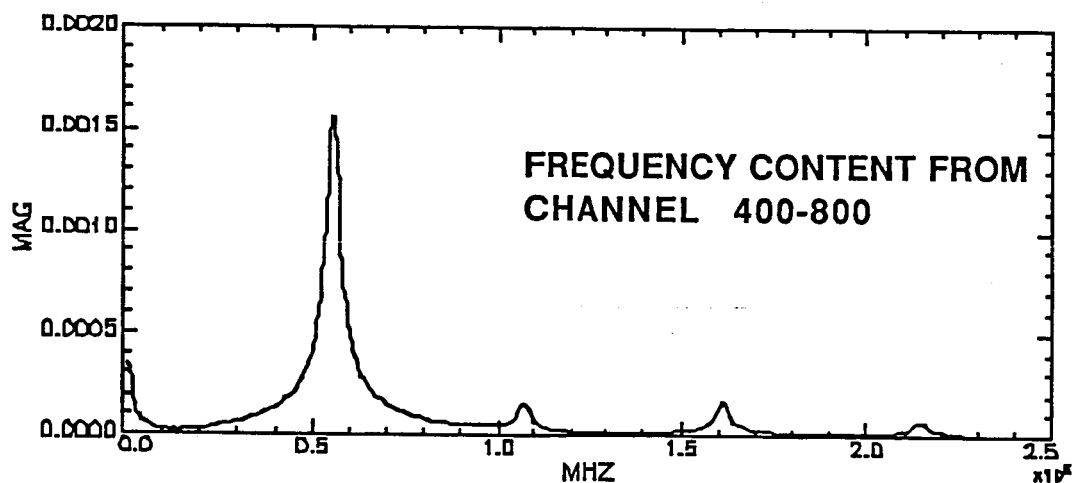
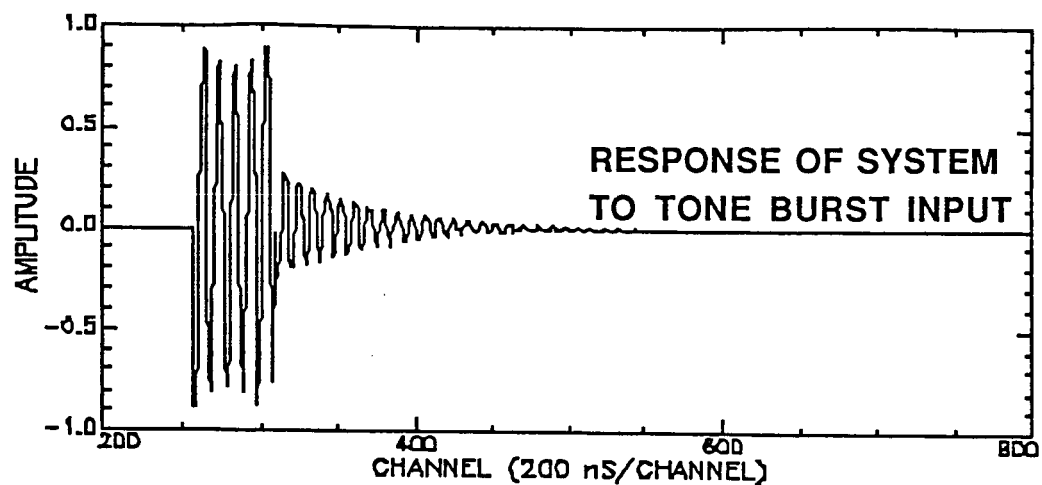


Figure 6.

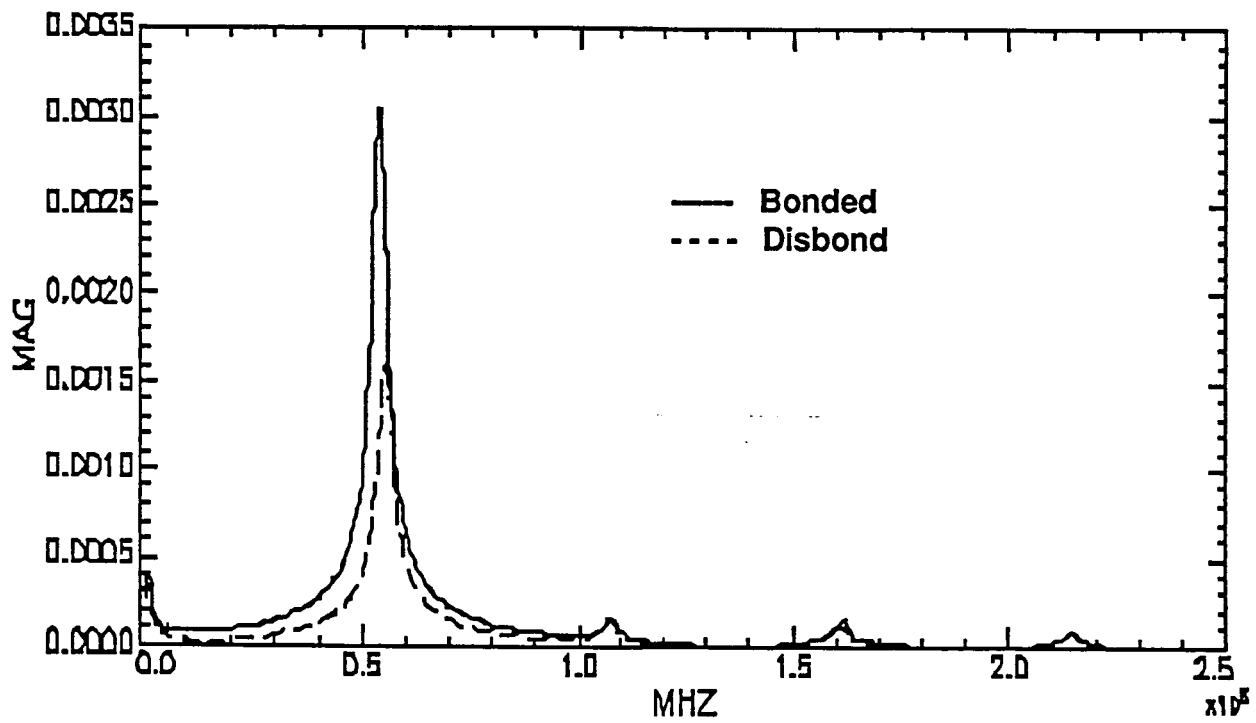
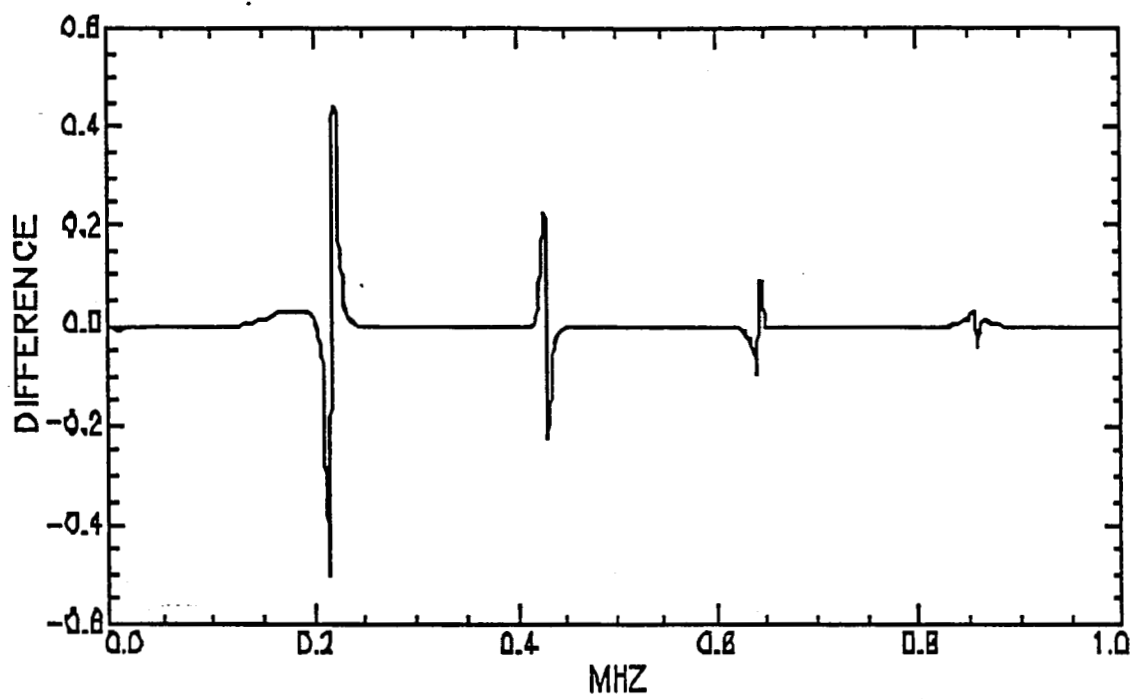


Figure 7. Frequency content in channels 400-800 for the case of — no disbond and - - - disbond between insulation (0.1") and propellant



**Figure 8. Difference in frequency response of multilayer resonators that are bonded and disbonded between the insulator (0.1") and propellant..**

# MODEL WITH BOND BETWEEN INSULATION (0.5") AND PROPELLANT

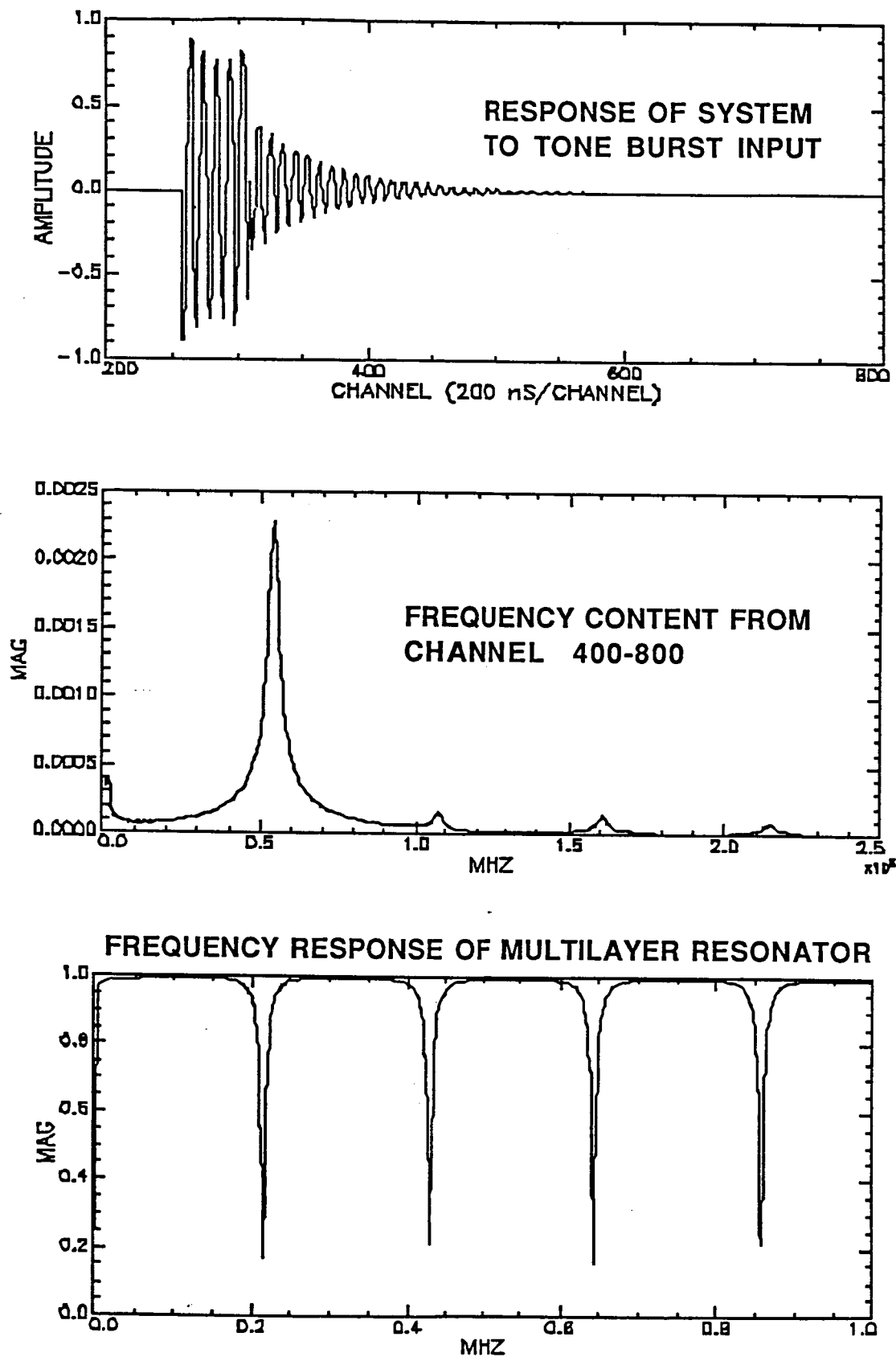


Figure 9.

# MODEL WITH DISBOND BETWEEN INSULATION (0.5") AND PROPELLANT

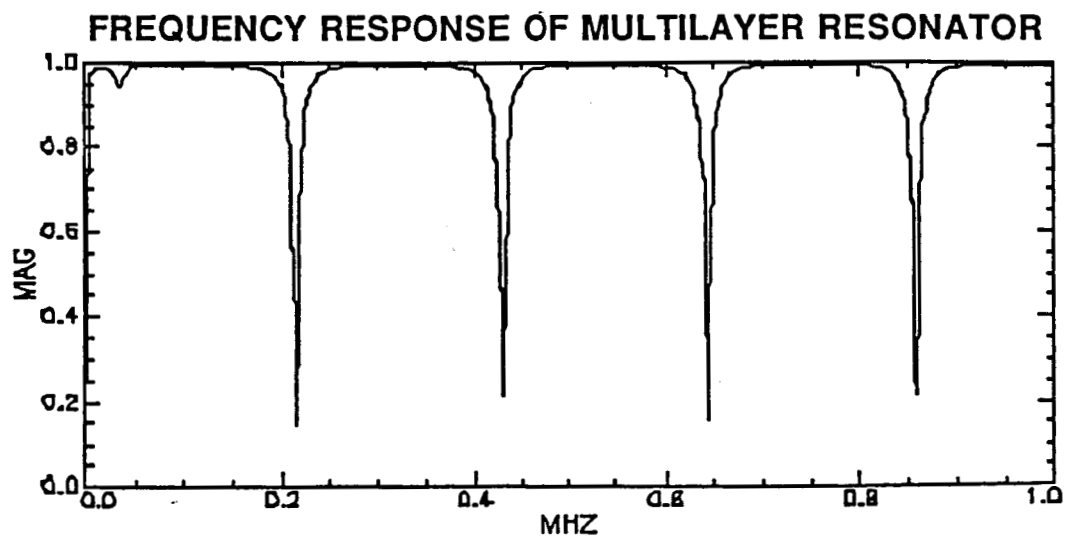
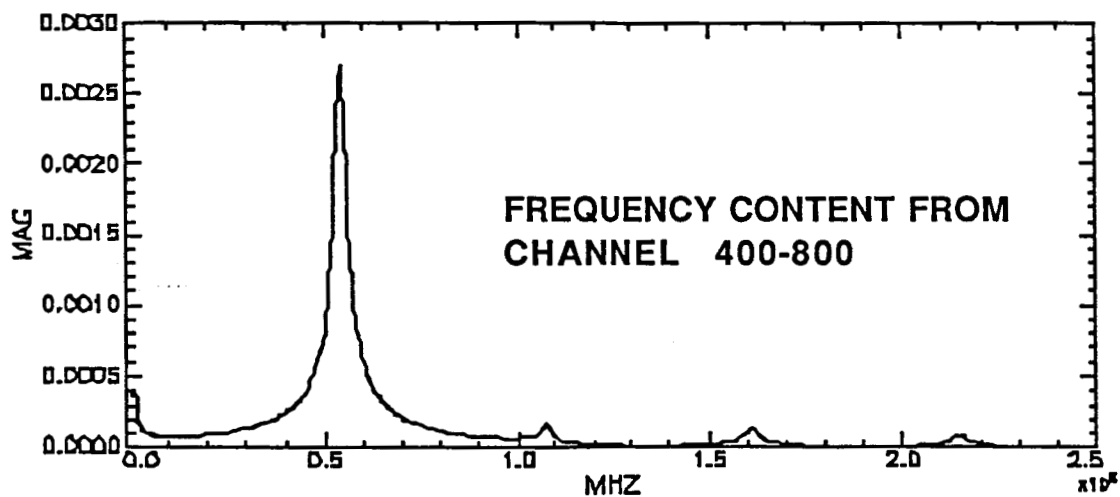
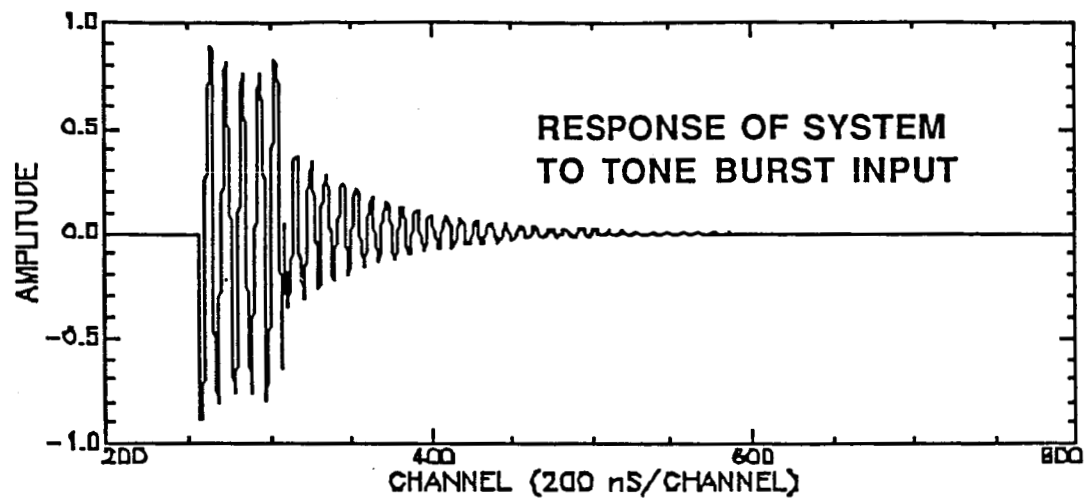


Figure 10.

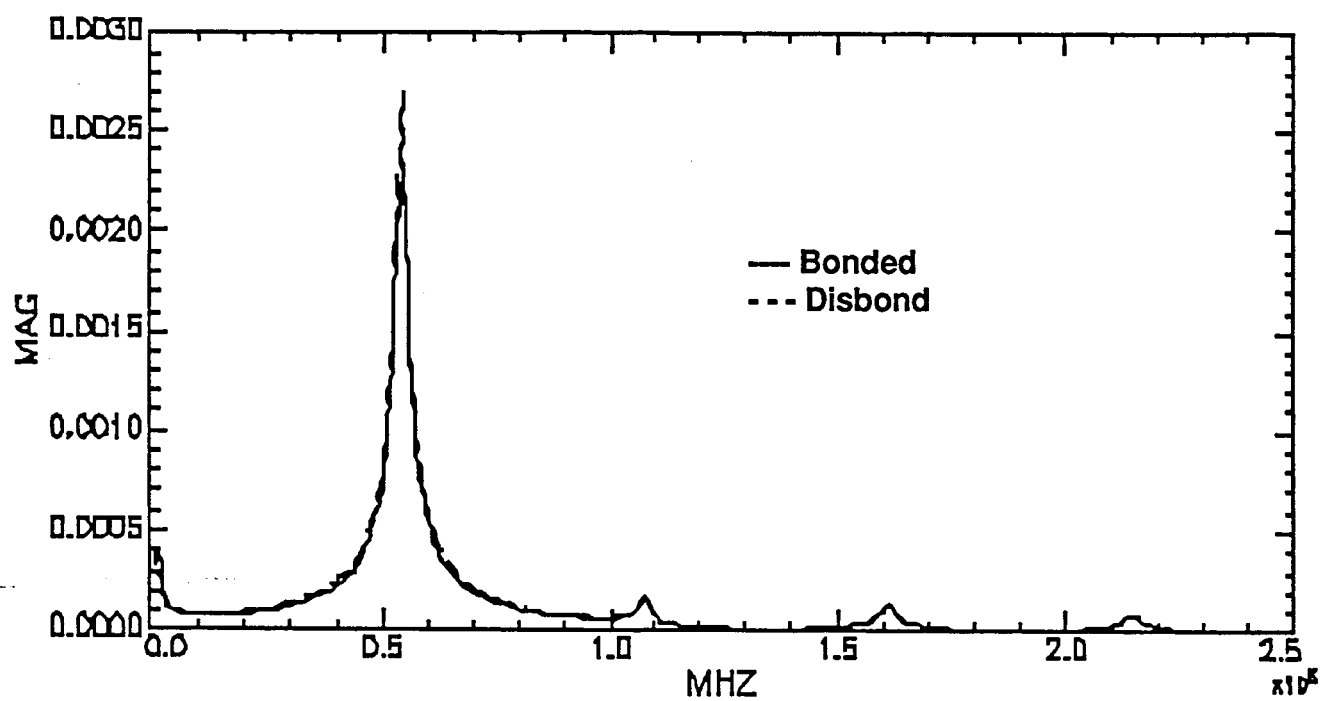
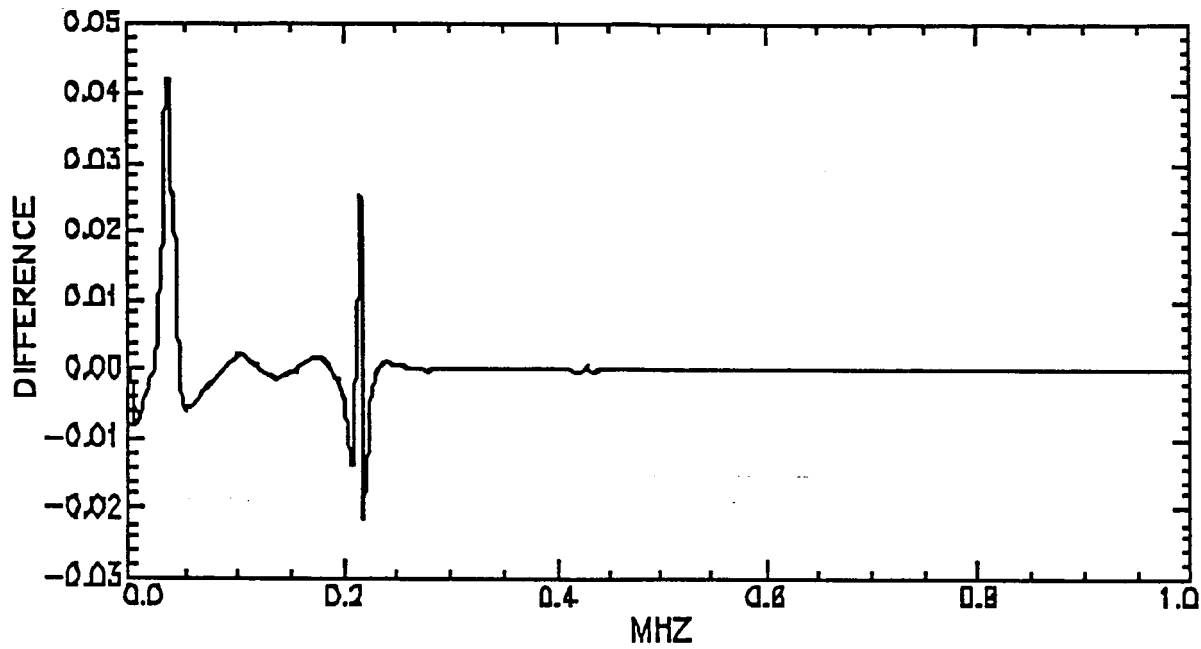


Figure 11. Frequency content in channels 400-800 for the case of — no disbond and - - - disbond between insulation (0.5") and propellant.



**Figure 12. Difference in frequency response of multilayer resonators that are bonded and disbonded between the insulator (0.5") and the propellant**

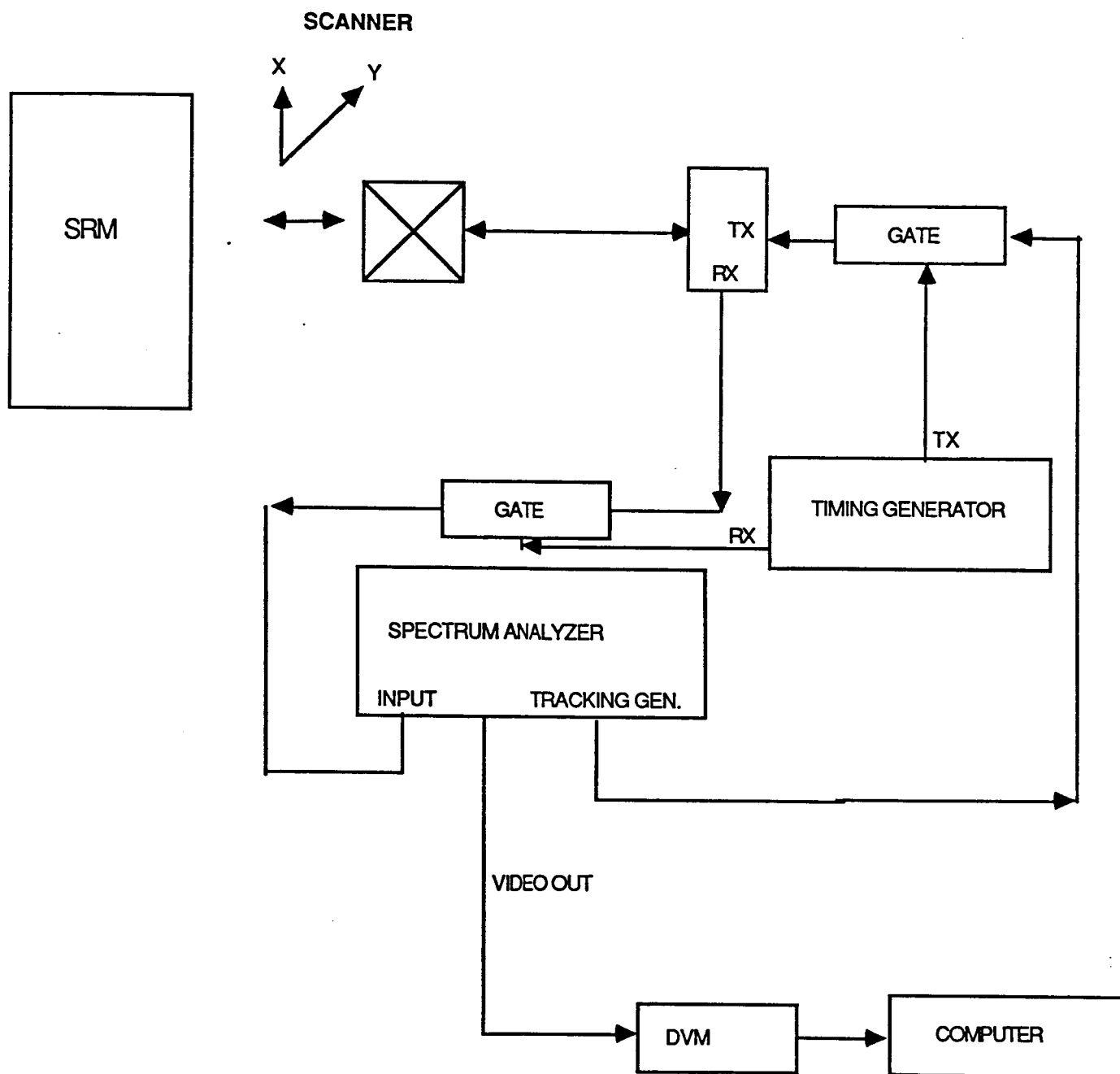


Figure 13.

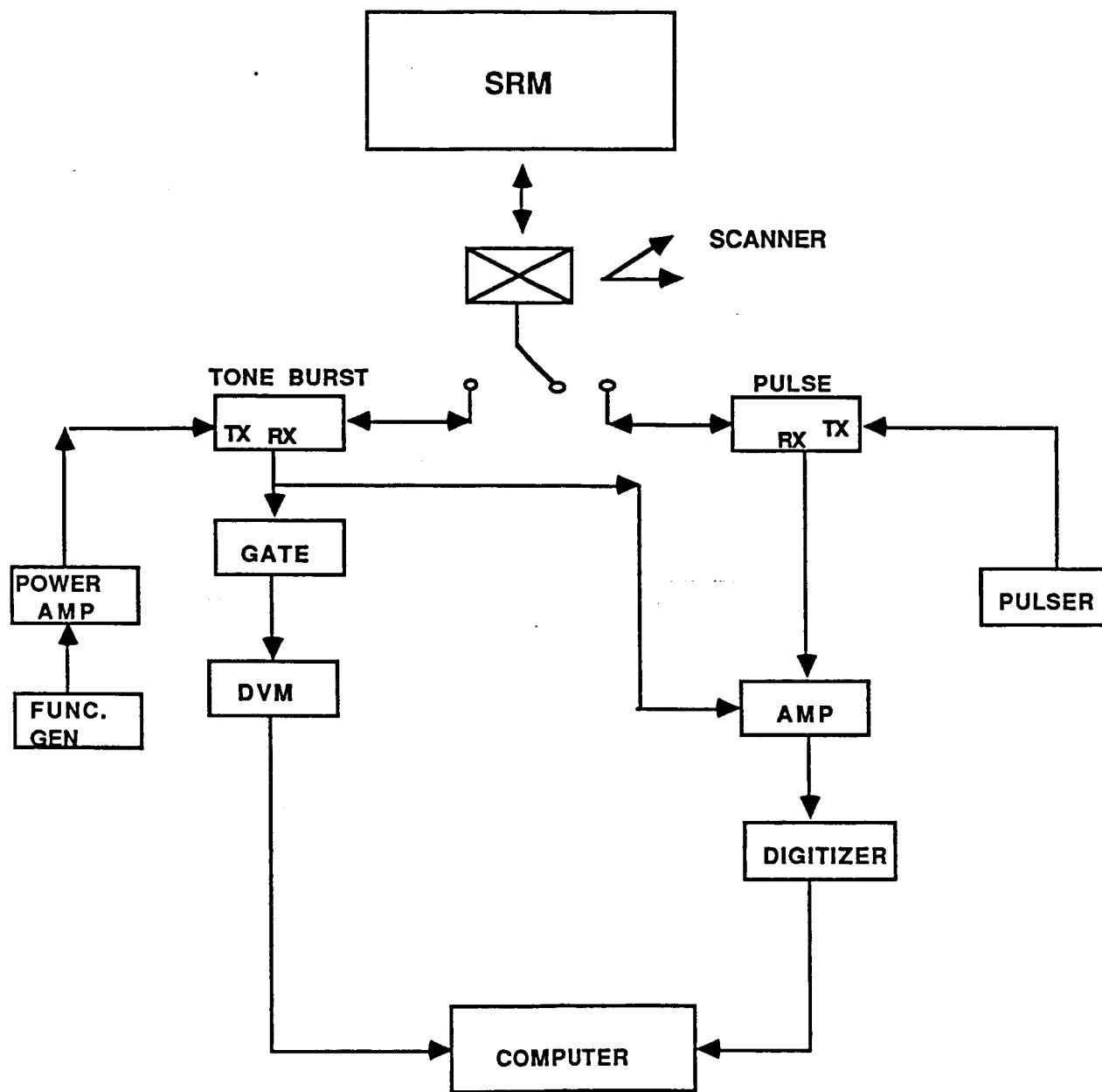


Figure 14.

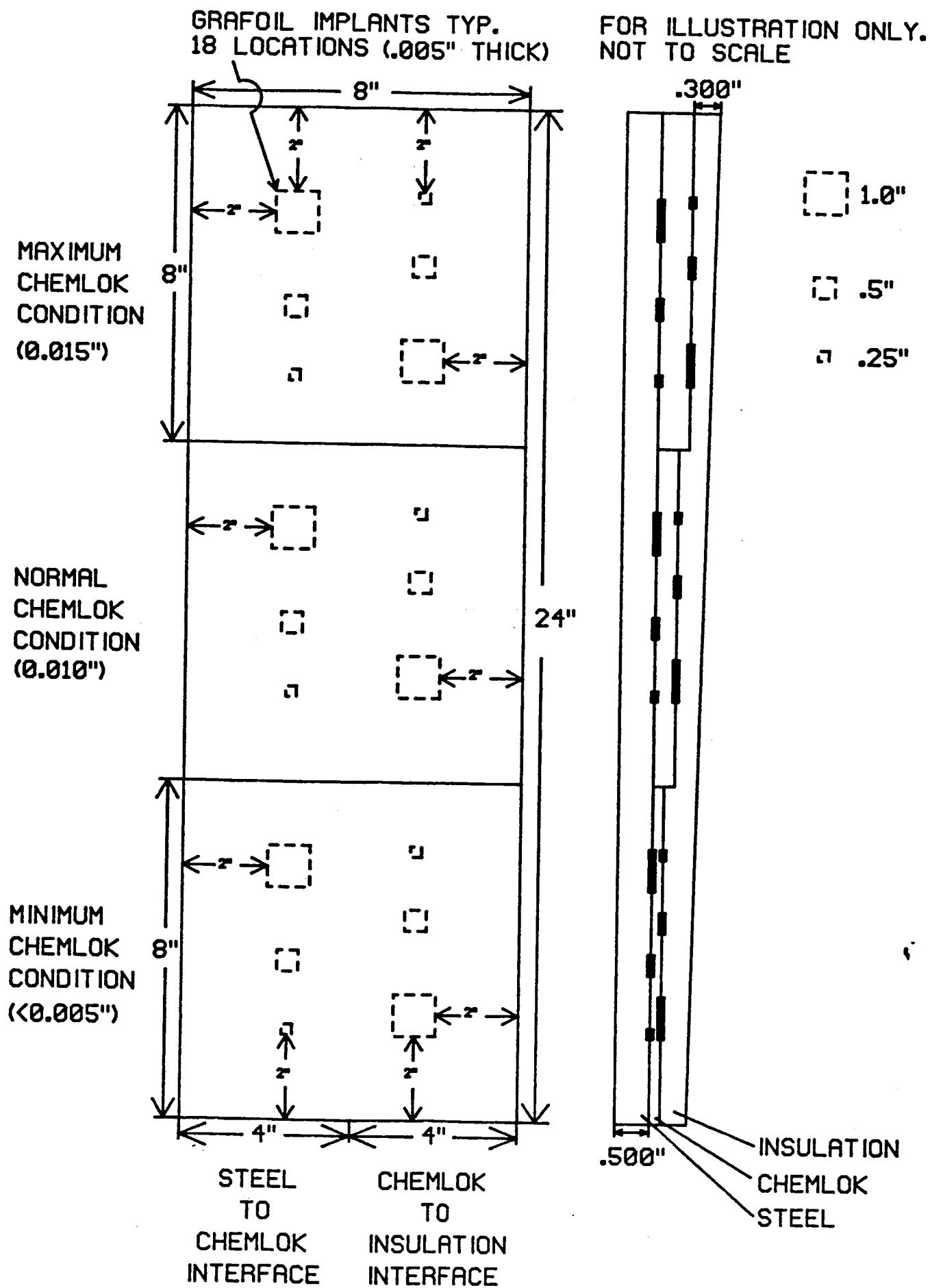


Figure 15.

ORIGINAL PAGE IS  
OF POOR QUALITY

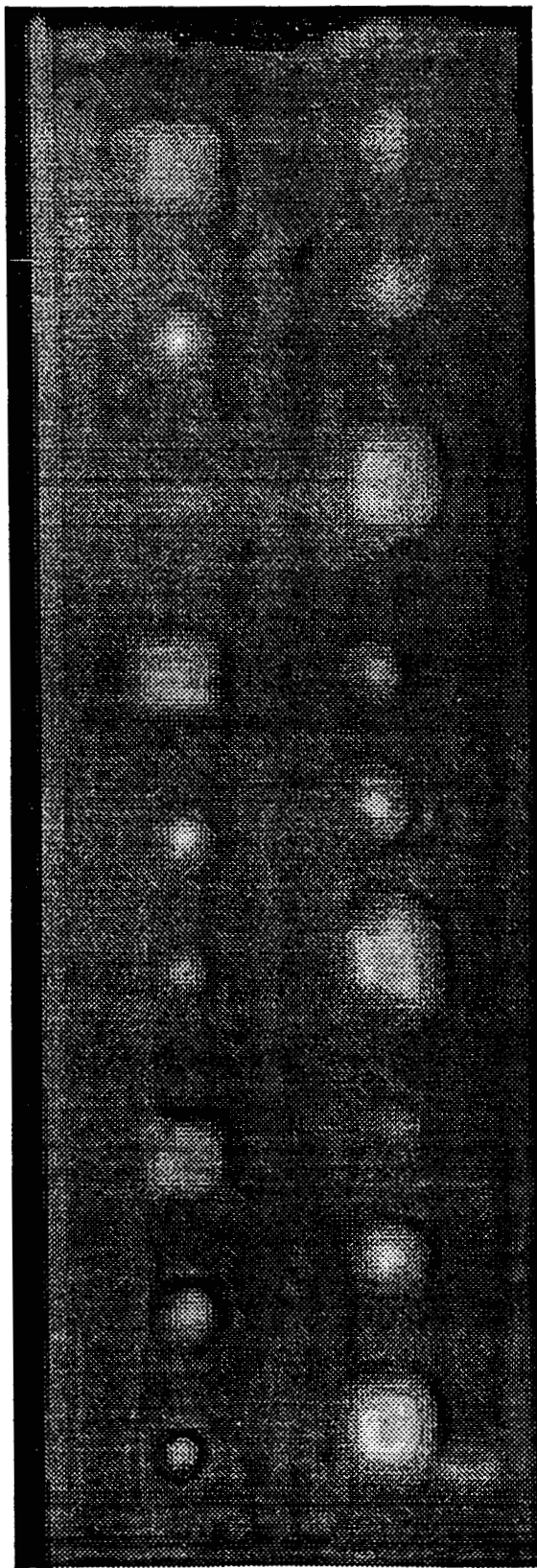
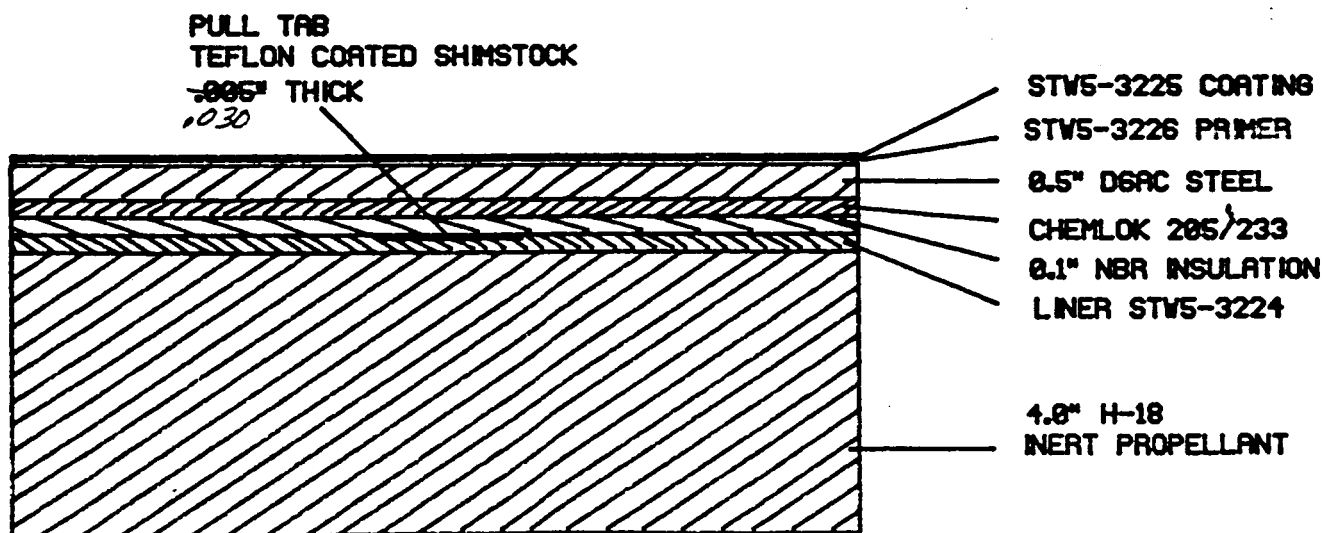
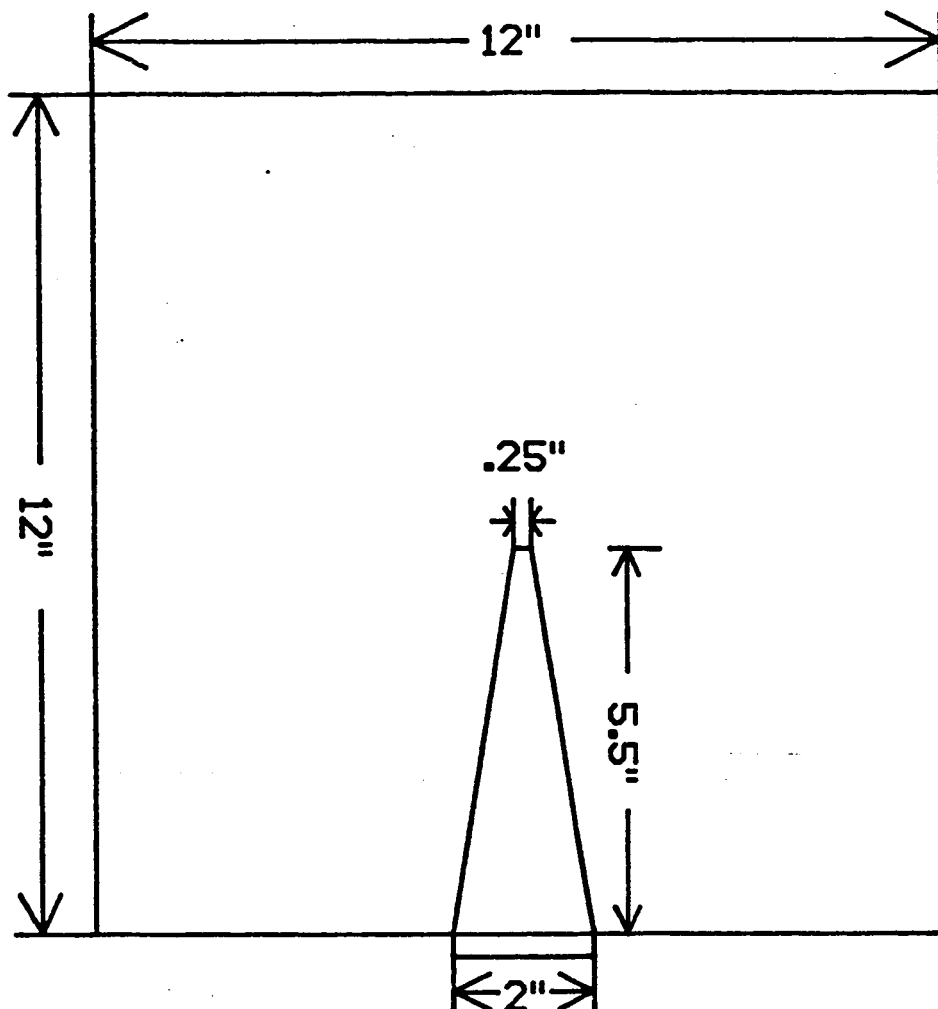


Figure 16.

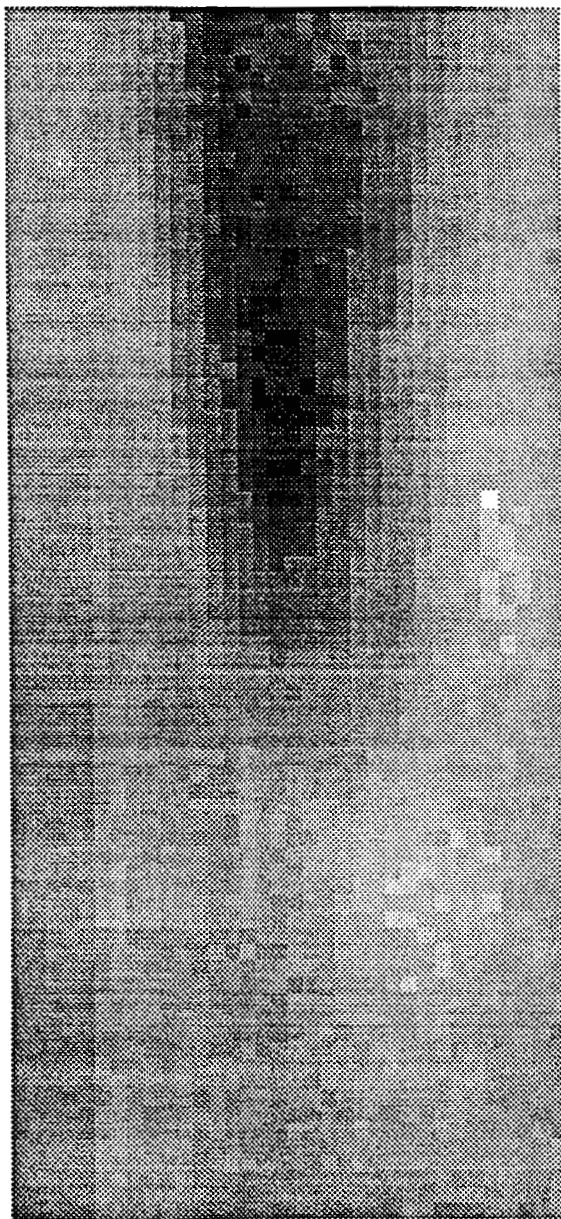
SPACE SHUTTLE UNBOND SAMPLE  
SRM-SAM8



UNBOND CONDITION IS LOCATED AT INSULATION-LINER INTERFACE

Figure 17.

Figure 18. Video out from Spectrum Analyzer at 500 kHz



ORIGINAL PAGE IS  
OF POOR QUALITY

Figure 19. 500 kHz Tone Burst-Peak Detected



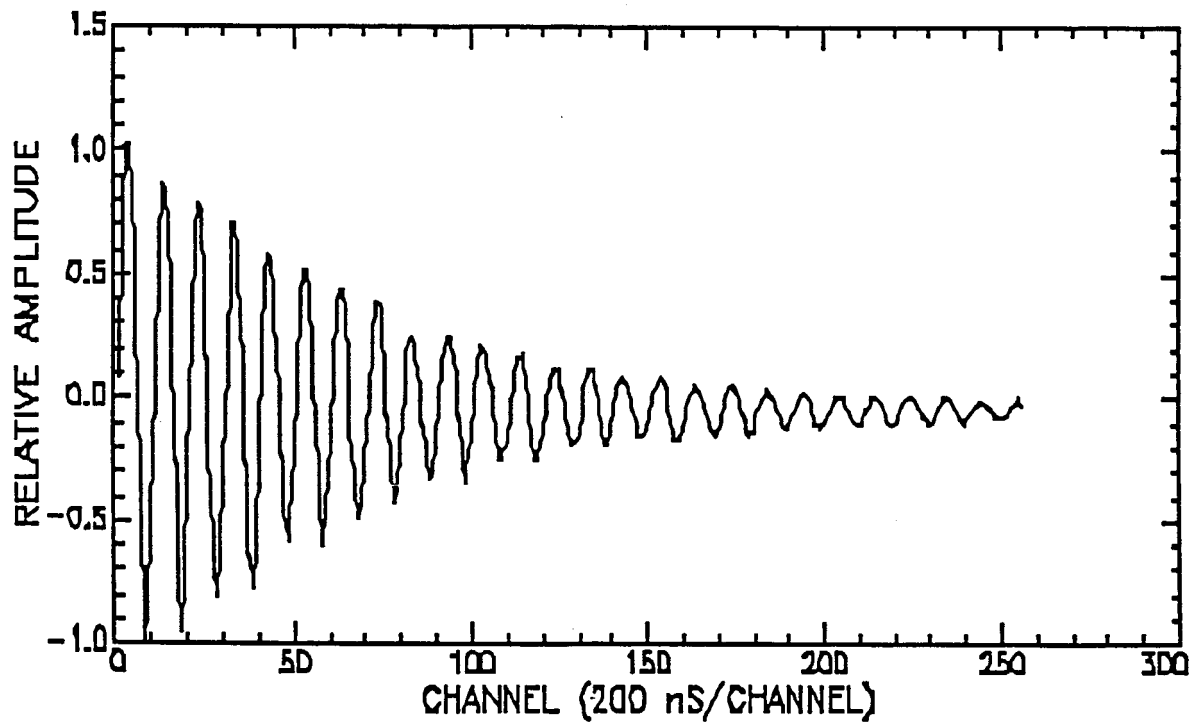


**Figure 20. Digitized waveform windowed by digitizer to include resonance decay . Acquired from bonded region of sample .**

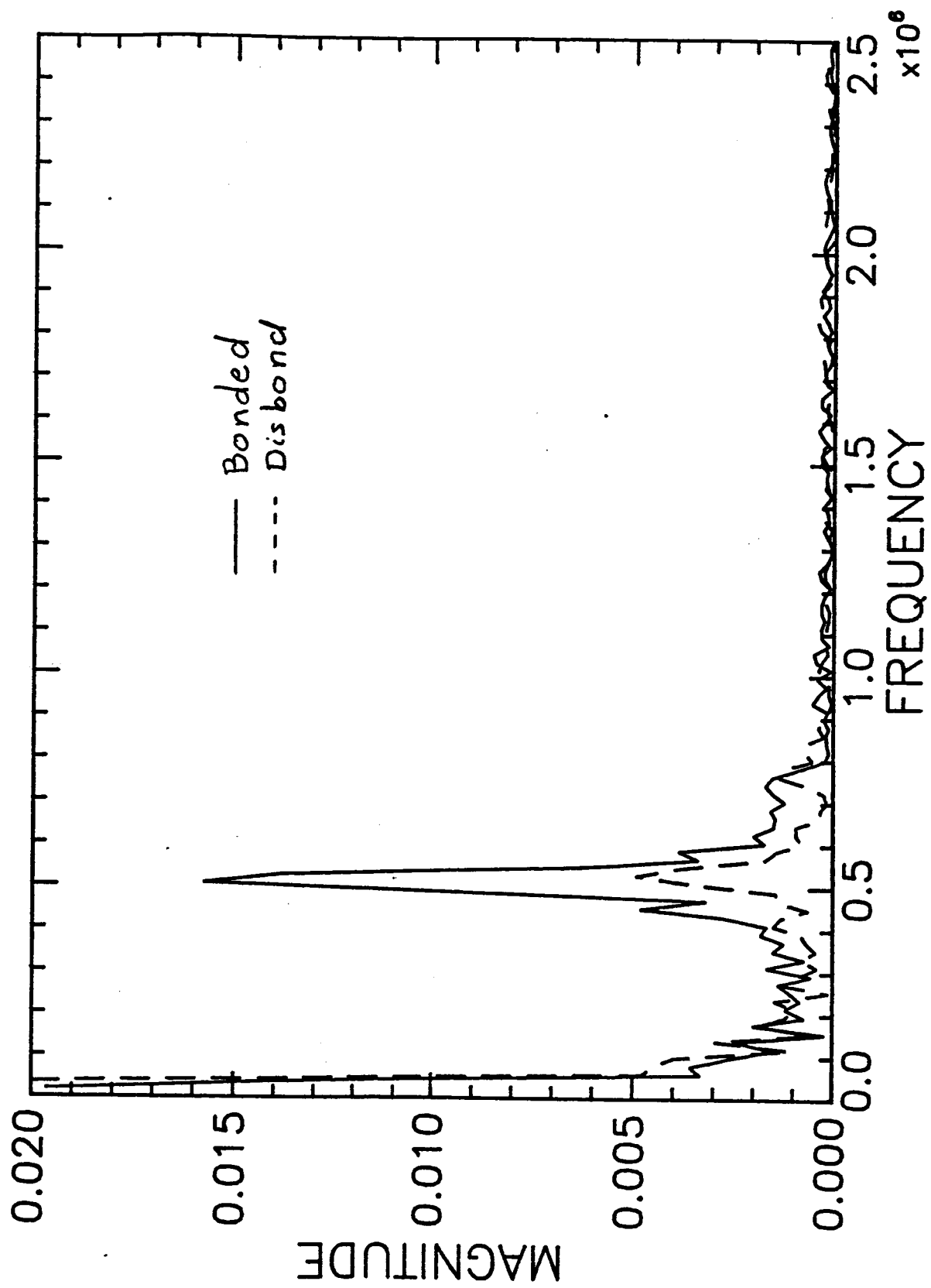
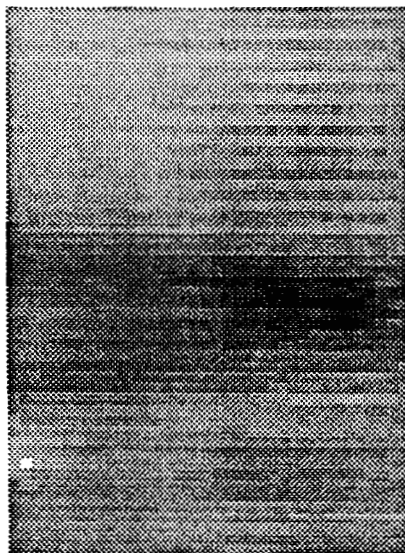


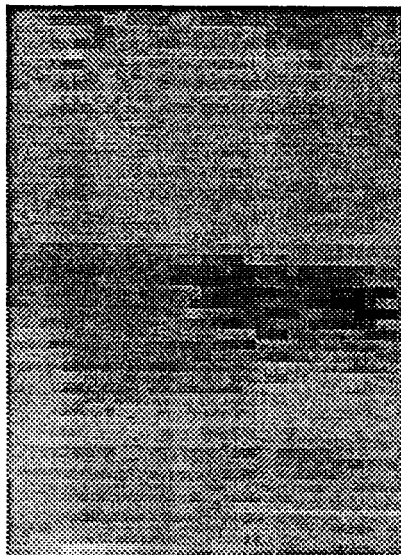
Figure 21

Figure 22. 500 kHz Tone Burst-Digitize-Frequency Window



ORIGINAL PAGE IS  
OF POOR QUALITY

Figure 23. Pulser-Digitize-Frequency Window



ORIGINAL PAGE IS  
OF POOR QUALITY

Figure 24. Pulse Input and Peak Detect

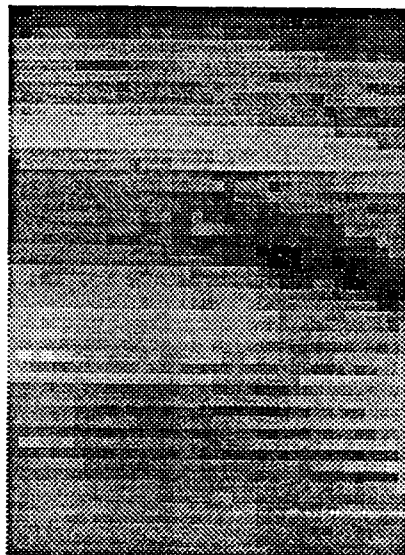
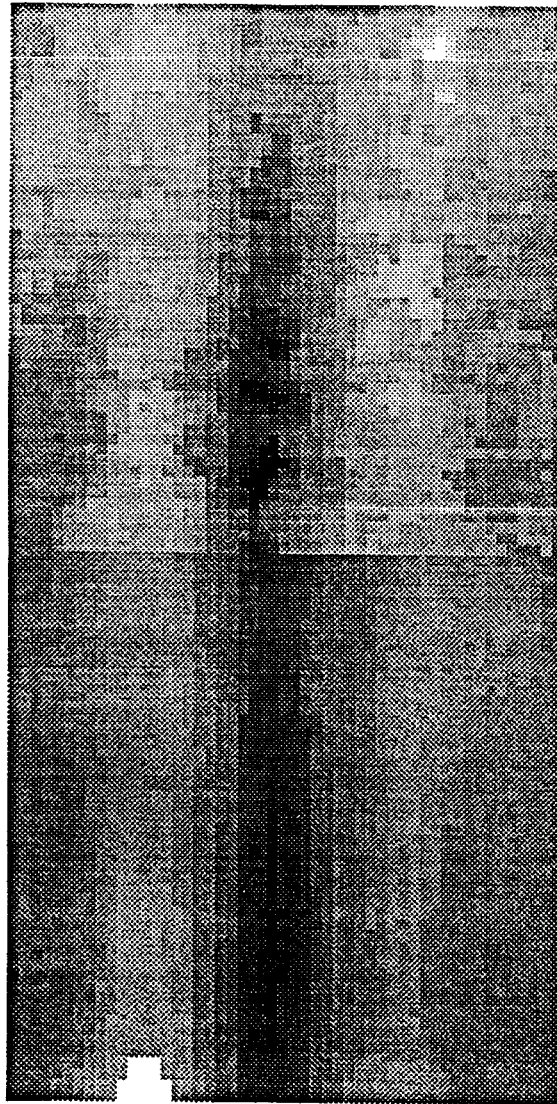


Figure 25.

ORIGINAL PAGE IS  
OF POOR QUALITY



L

I